targeted MS/MS was performed. Peaks lists were generated by the MassNavigator software package (Version 1.2.12; Mitsui Knowledge Industry, Tokyo, Japan) and searched against the NCBInr database (NCBInr_20120423.fast) using the Mascot software package (Version 2.2.1; Matrix Sciences, London, UK). The initial peptide tolerances in MS and MS/MS modes were ±0.05 and ±0.1 Da, respectively. The peptides were digested with trypsin, and up to one missed cleavage was allowed. The score threshold for achieving $P < 0.05$ was set by the Mascot algorithm on the basis of database size. If a peptide matched multiple proteins, then the protein name with the highest Mascot score was selected.

Immunohistochemistry for galectin-7

FFPE sections from all 86 cases were analyzed by quantitative immunohistochemistry (IHC). The 4-μm thick sections were incubated with a rabbit monoclonal anti-galectin-7 antibody (EPR4287; 1:2000; LifeSpan Biosciences, Inc., WA) for 60 min at room temperature. Then, they were incubated with biotinylated anti-primary antibodies (Histofine SAB PO kit; Nichirei, Tokyo, Japan). The signal was detected using streptavidin–peroxidase (Histofine SAB PO kit) and the diaminobenzidine tetrahydrochloride (DAB) substrate. Finally, the sections were counterstained with Mayer's hematoxylin and dehydrated.

Analysis of galectin-7 immunostaining

The galectin-7-stained area (G7S) was quantified by dividing the staining intensity of that area over the staining intensity of the whole tissue section using ImageJ (freeware available at http://rsb.info.nih.gov/nih-image/). The immunostaining pattern of the galectin-7 nuclear staining area (G7N) was defined by dividing the staining intensity of the galectin-7 immunostained area within the nucleus over G7S. The median G7N of the 18 learning samples was 0.168. Therefore, G7NL was graded as follows: weak (G7NL = 0; <0.15 of G7N), positive (G7NL = 1; 0.15–0.40 of G7N), or strongly positive (G7NL = 2; >0.40 of G7N), corresponding to highest tertile of the 18 learning samples.

Cell culture

The human oral SCC cell lines, HSC-3, HSC2, HOC313, HSC4, and Ho1-N-1, were established in the First and the Second Department of Oral and Maxillofacial Surgery, Faculty of Dentistry, Tokyo Medical and Dental University (Tokyo, Japan). SKN3 cells were purchased from the Japanese Collection of Research Bioresources (Osaka, Japan). HEK293 cells were purchased from DS Pharma Biomedical Co. Ltd. (EC85120602-FO; Osaka, Japan). These were maintained in Dulbecco's modified Eagle's medium (DMEM) containing a high concentration of glucose (4.5 mg/mL) supplemented with 10% fetal bovine serum (FBS) and cultured in a 5% CO_2 environment at 37°C.

Adenovirus vector

A cDNA for human *galectin-7* (Clone name: pFN21AE1213) was obtained from the Kazusa DNA Research Institute, Kisarazu, Japan (http://www.kazusa.or.jp). The adenoviral construct containing FLAG-tagged human galectin-7 (GAL7) was obtained using Adeno-X™ Adenoviral System 3 with tetracycline inducible expression system (Tet-On 3G Inducible) from Clontech (Mountain View, CA). FLAG (ATGGACTACAAGGACGACGATGACAAG) and human *galectin-7* sequences can be transferred as PCR products to the pAdenoX vector using the In-Fusion® cloning method (Clontech) according to the protocol. FLAG-tagged human *galectin-7* gene plus 15 bp of homology to pAdenoX vector was amplified using CloneAmp HiFi Premix (Clontech) with the following primers: 5′-GTAACTATAACGGTCATGGACTACAAGGACGACGATGACAAGATGTCCAACGTCCCCCACAAGTCCT-3′ (Ad-FLAG-GAL7 forward), 5′-ATTACCTCTTTCTCCTCAGAAGATCCTCACGGAGTCCAGCT-3′ (GAL7 reverse). The Pac I-Digested adenoviral construct was transfected into HEK293 cells. The virus was amplified and harvested according to the Clonetech protocol. The viral titer was determined by the Tissue Culture Infectious Dose 50 (TCID50) method. The infection was with the multiplicity of infection (MOI) of 0–100 IFU/cell in complete growth medium with or without 1 μg/mL doxycycline (Clontech).

Western blot analysis

Cells were lysed in a cell lysis buffer (20 mmol/L Tris-HCl pH 7.5, 1% Triton X-102, 0.1% SDS, 150 mmol/L NaCl, 1 mmol/L EDTA, 50 μg/mL Aprotinin and 80 μg/mL PMSF). The cell lysate was subjected to SDS-PAGE (sodium dodecyl sulfate polyacrylamide gel electrophoresis), followed by electroblotting onto polyvinylidene fluoride (PVDF) membranes. After blocking with 5% skim milk in phosphate-buffered saline (PBS) for 1 h, membranes were probed with specific a mouse monoclonal anti-FLAG (M2; 1:1000; Sigma, St. Louis, MO), a rabbit monoclonal anti-galectin-7 (EPR4287; 1:1000; LifeSpan Biosciences, Inc.), a rabbit polyclonal anti-caspase-3 (#9662; 1:1000; Cell Signaling Technology, Inc., MA), and a rabbit monoclonal anti-beta-actin (#8457(D6A8); 1:1000; Cell Signaling Technology, Inc.) antibodies. Immunoreactive

signals were visualized by SuperSignal® west dura extended duration (Thermo Scientific, Waltham, MA), using Light-capture® (ATTO, Bioscience and Biotechnology, Tokyo, Japan).

In vitro cell viability assay

Cell viability was assessed by the colorimetric water-soluble tetrazolium salt (WST) assay (Cell counting kit- 8; Dojindo Laboratories, Kumamoto, Japan) as described by the manufacturer. Briefly, cells (1×10^4/well) were seeded into 96-well plates and cultured for 12 h. Then, cells were incubated with adenovirus infection for 12 h with or without 1 μg/mL doxycycline, and further cultured with or without doxycycline in fresh medium with the absence or presence of anticancer drug, 5 μg/mL cisplatin or 50 μg/mL 5-fluorouracil, for an additional 24 h. At the end of the culture period, 10 μL of a formazan-generating reagent, WST-8, was added to each well for 60 min at 37°C. The absorbance of each well at 450 nm was then measured using a microplate reader.

Statistical Analysis

The MS data and cell viability were analyzed by receiver operating characteristic (ROC) curve analysis, including area under the curve (AUC), stepwise discriminant analysis, *T*-tests, Mann–Whitney *U*-tests, and two-sided log-rank tests with PASW Statistics, version 18 (SPSS Inc., Chicago, IL). $P < 0.05$ was considered statistically significant.

Results

Identification of a predictive marker of chemotherapy and/or radiotherapy resistance in OSCC by LC-MS

To identify a predictive marker of chemotherapy and/or radiotherapy resistance in OSCC, 18 biopsy samples, including nine samples from Group R and nine samples from Group S, were analyzed by LC-MS (Fig. 1). A total of 70,510 peaks per sample were readily detected and quantified. Among them, 10,869 MS peaks differed in intensity between Group R and Group S ($P < 0.05$; AUC >0.7). We further selected 105 peaks with Mascot scores >50 and excluded abundant proteins, including keratin, fibrinogen, collagen, and histone. Among them, we selected 20 peaks with Group R/Group S peak intensity ratios ≤0.5. We further limited our selection to the peaks with high predictive power on the basis of discriminant analysis (stepwise method), which identified two candidate peaks (ID1181 and ID2504). We chose the peak with the highest Mascot score: ID1181 (Table 2). MS/MS spectra of the ID1181 peaks matched the amino acid sequence of the galectin-7 protein.

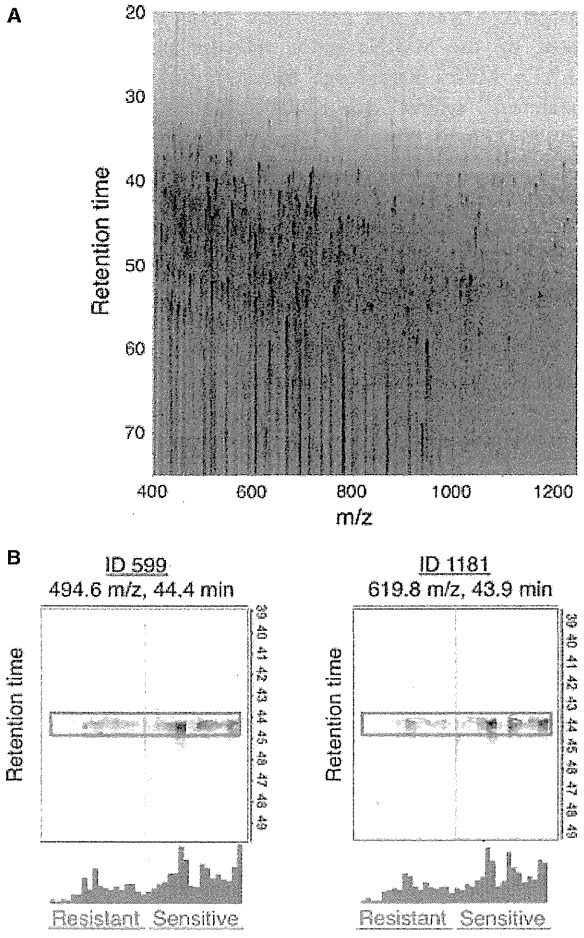

Figure 1. Identification of proteins differentially expressed in OSSC samples from patients sensitive (Group S) or resistant (Group R). The samples were processed by LC-MS and analyzed with 2DICAL. (A) Two-dimensional display of a representative sample. (B) Separation gel for the MS peaks ID599 and ID1181 from each group ($N = 18$). Group R (red) exhibits lower expression of the two peaks compared with Group S (blue).

Expression of galectin-7 in OSCC by IHC

The protein expression of galectin-7 in OSCC tissue was confirmed by IHC analysis of the FFPE samples used for LC-MS analysis (Fig. 2A). Pearson's correlation analysis was conducted between G7S and each of the peaks listed in Table 2. A significant positive correlation was detected between G7S and the intensity of the two galectin-7 peaks, namely ID599 ($r = 0.71$; $P = 0.001$; Fig. 3A) and ID1181 ($r = 0.73$; $P = 0.001$; Fig. 3B). Scatter plot

Table 2. List of peptides that differed between the resistant group and sensitive group.

ID	M/Z	RT	Charge	Ratio (R/S)	UniProt accession number	Protein Description	Mascot score	Peptide sequence	Resistant (mean ± SD)	Sensitive (mean ± SD)
4722	725.7	55.3	3	0.47	P31947	14-3-3 protein sigma	62.41	TTFDEAMADLHTLSEDSYK	1070 ± 538	2263 ± 846
6326	776.4	55.3	2	0.48	P04083	Annexin A1	62.79	GTDVNVFNTILTTR	2782 ± 1387	5762 ± 3858
25210	574.0	38.9	3	0.25	P22528	Cornifin-B	51.67	QPCTPPPQLQQQQVK	71 ± 83	282 ± 293
1294	726.7	57.3	3	0.48	P15924	Desmoplakin	129.32	FLEFQYLTGGLVDPEVHGR	1805 ± 1148	3765 ± 2017
2504	627.8	50.5	2	0.39	P15924	Desmoplakin	60.97	AITGFDDPFSGK	958 ± 348	2460 ± 938
3011	843.5	50.8	2	0.45	P15924	Desmoplakin	116.28	ITNLTQQLEQASIVK	846 ± 351	1889 ± 751
3292	752.1	55.7	3	0.48	P15924	Desmoplakin	105.46	LLEAQIASGGVVDPVNSVFLPK	1109 ± 568	2304 ± 930
1196	677.4	52.3	2	0.47	P12724	Eosinophil cationic protein	63.88	YPVVPVHLDTTI	1297 ± 443	2786 ± 1933
599	494.6	44.4	3	0.45	P47929	Galectin-7	52.89	SSLPEGIRPGTVLR	2730 ± 1558	6018 ± 2658
1181	619.8	43.9	2	0.47	P47929	Galectin-7	87.57	LDTSEVVFNSK	1763 ± 993	3764 ± 1639
31232	593.6	48.5	2	0.42	P01857	Ig gamma-1 chain C region	57.90	GPSVFPLAPSSK	192 ± 225	453 ± 169
1316	618.9	51.4	2	0.46	P14923	Junction plakoglobin	87.37	VSVELTNSLFK	1815 ± 1296	3931 ± 1850
914	576.8	52.3	2	0.42	P05164	Myeloperoxidase	56.64	IANVFTNAFR	925 ± 727	2198 ± 1956
20233	576.8	52.7	2	0.48	P05164	Myeloperoxidase	56.77	IANVFTNAFR	659 ± 404	1365 ± 778
2998	688.9	46.5	2	0.47	Q13835	Plakophilin-1	66.93	VMGNQVFPEVTR	1035 ± 781	2190 ± 1187
10288	594.3	37.7	2	0.42	Q13835	Plakophilin-1	85.89	LLQSGNSDVVR	413 ± 235	987 ± 597
26579	450.7	36.8	2	0.49	Q13835	Plakophilin-1	50.69	LDAEVPTR	261 ± 181	538 ± 346
1257	582.0	46.1	3	0.48	P06702	Protein S100-A9	65.32	VIEHIMEDLDTNADK	1365 ± 945	2817 ± 1354
2735	807.9	66.0	2	0.48	P06702	Protein S100-A9	111.26	QLSFEEFIMLMAR	829 ± 807	1743 ± 1423
9832	744.3	42.5	2	0.49	P68363	Tubulin alpha-1B chain	87.43	LISQIVSSITASLR	426 ± 143	870 ± 572

RT, retention time; Ratio (R/S), a ratio of average peak intensity in the resistant group to that in the sensitive group.

analysis was conducted for the G7S values of Group R and Group S (Fig. 4A). The median G7S was significantly lower for Group R (0.455) than for Group S (0.666; Mann–Whitney *U*-test; $P = 0.003$), suggesting that oral SSC patients with low galectin-7 expression are more likely to exhibit chemotherapy and/or radiotherapy resistance. The sensitivity of this prediction was 88.9% and specificity was 88.9% (cutoff point: 0.526).

A careful observation of the IHC findings revealed that galectin-7 was expressed in both the cytosolic and nuclear compartments; we observed strong nuclear staining in Group R and mostly cytosolic staining in Group S (Fig. 2). Median G7N was 10-fold higher for Group R than for Group S, with 0.549 and 0.042, respectively (Mann–Whitney *U*-test; $P = 0.003$; Fig. 4B). These data show that chemotherapy and/or radiotherapy resistance is associated with a nuclear concentration of galectin-7. Therefore, we conducted a discriminant analysis using G7S and G7NL for the 18 learning samples analyzed by LC-MS and IHC and obtained the following predictive formula for chemotherapy and/or radiotherapy resistance:

$$\text{Galectin-7 prediction score (G7PS)} = 5.812\text{G7S} - 1.246\text{G7NC} - 1.96\,(\text{cutoff point} : 0)$$

Based on this formula, the sensitivity of prediction was 100% and specificity was 88.9%, indicating that sensitivity was increased in the 18 learning cases (Fig. 5A). When this formula was used to analyze the remaining 68 test cases, the sensitivity of prediction was 96.0% and specificity was 39.5% (Fig. 5B).

Galectin-7 prediction score correlates with poor prognosis in patients with OSCC

Five-year cumulative survival rates in Group S and Group R were estimated by Kaplan–Meier analysis using galectin-7 as a predictor of chemotherapy and/or radiotherapy resistance. The cumulative 5-year disease-specific survival rate was 75.2% in patients with resistant prediction using galectin-7 prediction score (G7PS) (<0) and 100% in patients with sensitive prediction (G7PS ≥0; Fig. 6). There was a significant positive correlation between resistant

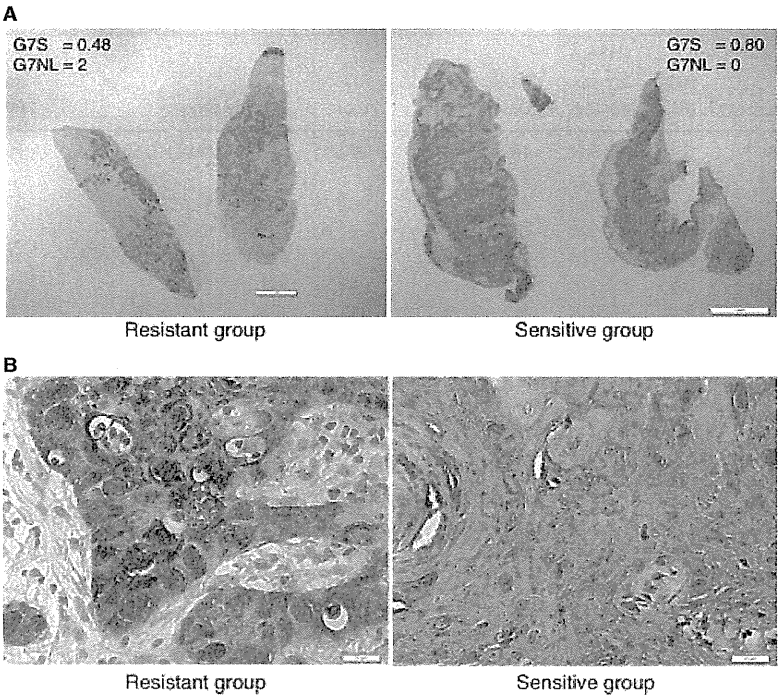

Figure 2. Immunohistochemistry of galectin-7. (A) Low magnification (bar: 1 mm) showing the overall staining intensity and distribution. Left panel: galectin-7 staining area (G7S) = 0.48, galectin-7 nuclear staining level (G7NL) = 2. Right panel: G7S = 0.80, G7NL = 0. (B) High magnification (bar: 20 μm) showing galectin-7 was expressed in both the cytosolic and nuclear compartments; we observed strong nuclear staining in Group R and mostly cytosolic staining in Group S.

prediction using G7PS and survival parameter (log-rank test; $P = 0.027$; Fig. 6).

Galectin-7 decreases cell viability

To investigate the roles of galectin-7 in OSCC cells, the expression status of galectin-7 in six human OSCC cell lines was detected by Western blot analysis. A low endogenous expression of galectin-7 was detected in all OSCC cell lines except SKN3 (Fig. 7A). Next, we examined the effect of overexpressed galectin-7 in OSCC cells. HSC3 cells were infected with recombinant adenovirus encoding FLAG-tagged galectin-7 (Ad-FLAG-GAL7). The expression of galectin-7 was detected in a MOI-dependent manner with 1 μg/mL doxycycline by Western blot analysis (Fig. 7B), and we confirmed that FLAG-tagged galectin-7 was strongly expressed in HSC3 cells than endogenous expressions of galectin-7 in SKN3 or HSC2 cells (Fig. 7C). To examine the infection efficiency and intracellular distribution of Ad-FLAG-GAL7, we performed immunofluorescence labeling for overexpressed galectin-7. The infection efficiency of Ad-FLAG-GAL7 in HSC3 cells at MOI 50 was ~80% (Fig. S1A). The intracellular distribution of Ad-FLAG-GAL7 was similar to the IHC staining pattern of galectin-7 (Fig. 8B). Moreover, by Western blot analysis, we confirmed that analysis of supernatants from HSC3 cells infected with Ad-FLAG-GAL7 or other OSCC cell lines have failed to provide evidence for a secreted form of galectin-7 (data not shown). To examine the effect of galectin-7 on cell viability, HSC3 cells infected with Ad-FLAG-GAL7 (MOI of 50) were cultured for 24 h with or without doxycycline. The overexpression of galectin-7 significantly decreased cell viability in normal culture conditions (Fig. 8A). Furthermore, similar results were observed when we treated the cells with 5 μg/mL cisplatin or 50 μg/mL 5-fluorouracil (Fig. 8A). These results indicate that galectin-7 may be involved in tumor cell proliferation/viability rather than chemosensitivity. We also investigated the role of galectin-7 using antisense galectin-7 oligonucleotides in OSCC cell lines. Unfortunately, the results showed no effects of galectin-7 knockdown on cell viability (Fig. S2). To determine whether the decreased cell viability was because of apoptosis, Ad-FLAG-GAL7-infected HSC3 cells were cultured with or without doxycycline. We observed weak activation and cleavage of caspase-3 induced by the overexpression of galectin-7 was observed (Fig. 8B) indicating that the decreased cell

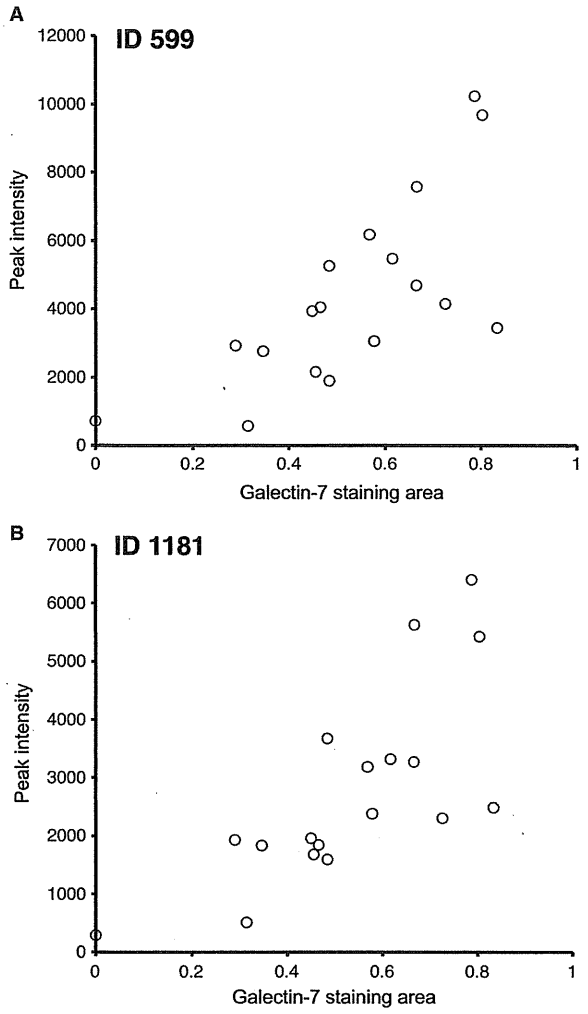

Figure 3. Regression analysis between the galectin-7 staining area (G7S) and the intensity of the MS peaks. Significant positive correlations were detected for both peaks, namely (A) ID599 ($r = 0.71$; $P = 0.001$) and (B) ID1181 ($r = 0.73$; $P = 0.001$).

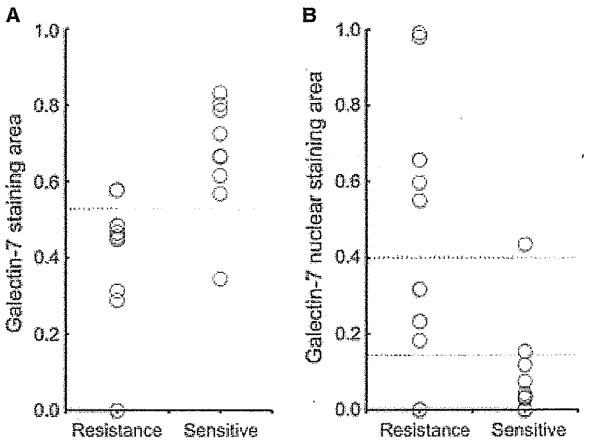

Figure 4. Scatter plot analysis for galectin-7 immunostaining. The two groups were compared for quantitative values of (A) galectin-7 staining area (G7S) and (B) galectin-7 nuclear area (G7N). Median G7S was lower for Group R than for Group S, but median G7N was 10-fold higher for Group R than Group S. Classification values for the galectin-7 nuclear staining area are shown by the horizontal lines as values of 0.15 and 0.40.

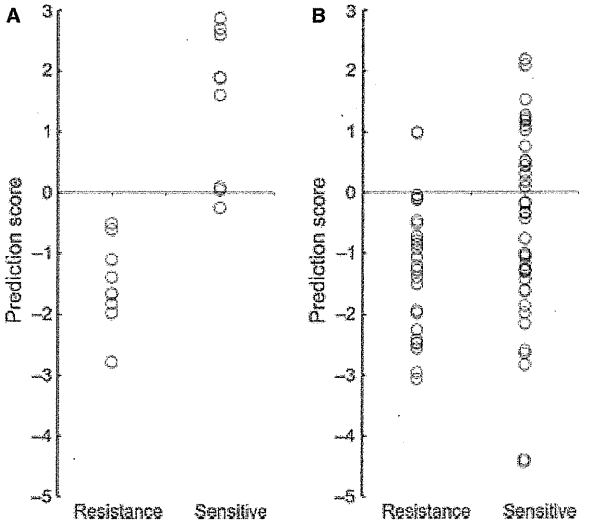

Figure 5. Scatter plot analysis for the galectin-7 prediction score (G7PS). (A) In the learning cases. (B) In the test cases.

viability by overexpression of galectin-7 may be because of growth arrest rather than apoptosis.

Discussion

The identification of tumor response predictors applying to a variety of radiotherapy and chemotherapy regimens will allow oncologists to customize strategies aimed at minimizing exposure to high-dose adjuvant therapy. To identify candidate biomarkers from the proteomics data, we used the 2DICAL analysis platform that performs a quantitative comparison of unlabeled shotgun proteomics data generated by LC-MS [11]. This approach was successfully used to identify blood biomarkers in pancreatic and colorectal cancer patients [12–17]. The use of proteins extracted from FFPE tissues in the form of tryptic peptides is compatible with a variety of MS-based proteomics [8]. However, we present the first report, as per our knowledge, on tumor response predictors in patients with OSCC.

Galectins constitute a family of evolutionary-conserved carbohydrate-binding proteins. They are widely distrib-

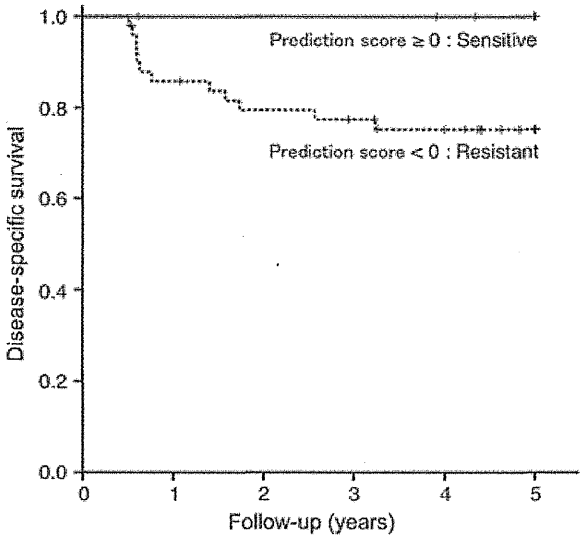

Figure 6. Kaplan–Meier survival analysis based on G7PS. There was a significant correlation between resistant prediction and survival parameter (log-rank test; $P = 0.027$).

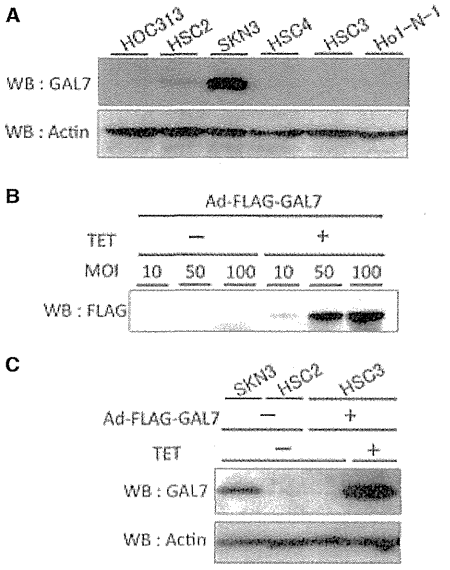

Figure 7. Adenovirus-mediated expression of galectin-7 in oral SCC cell lines. (A) Endogenous expression of galectin-7 in oral SCC cell lines. (B) Adenovirus-mediated expression of galectin-7 in HSC3 cells. HSC3 cells were infected with the indicated MOI of a recombinant adenovirus encoding FLAG-tagged galectin-7 (Ad-FLAG-GAL7) with or without 1 μg/mL doxycycline. (C) FLAG-tagged galectin-7 in HSC3 cells strongly expressed rather than endogenous expressions of galectin-7 in SKN3 or HSC2 cells. HSC3 cells were infected with MOI 50 of Ad-FLAG-GAL7. Then, SKN3, HSC2 and HSC3 cells were cultured with or without doxycycline in fresh medium for 24 h. The lysates were analyzed by Western blot analysis.

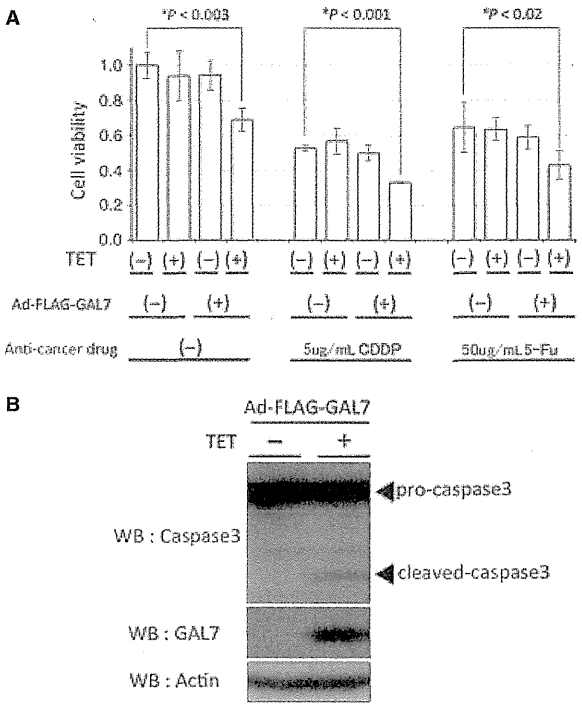

Figure 8. Overexpression of galectin-7 decreased cell viability. (A) Effect of galectin-7 in HSC3 cells. HSC3 cells were infected with Ad-FLAG-GAL7 at MOI 50. Then, cells were cultured with or without doxycycline in a fresh medium with the absence or presence of anticancer drug, 5 μg/mL cisplatin or 50 μg/mL 5-fluorouracil. Cell viability was assayed as described in Patients and Methods. Data represent the means ± SD of four independent experiments. $^*P < 0.05$, compared with uninfected cells in the absence of anticancer drugs. 5-Fu, 5-fluorouracil; CDDP, cisplatin; TET, doxycycline. (B) Cleavage of caspase-3 induced by the overexpression of galectin-7. HSC3 cells were infected with Ad-FLAG-GAL7 at MOI 50. Then, cells were cultured with or without doxycycline in a serum-free medium for 36 h. The lysates were analyzed by Western blot analysis. Beta-actin was used as a loading control.

uted in all organisms and are implicated in many essential functions such as development, differentiation, cell–cell adhesion, cell–matrix interaction, growth regulation, and apoptosis [18]. The various roles of galectins in cancer invasion and metastasis have been well documented [19, 20]. However, very little is known about how galectin-7 expression affects cancer progression [18]. The expression level of galectin-7 varies widely among tumor types, from completely downregulated to highly upregulated [21–24]. De novo galectin-7 expression by p53 is associated with apoptosis, which inhibits tumor growth [25]. Alternatively, galectin-7 mediates the nuclear export of Smad3 through complex formation, which is essential for the tumor-suppressive effects of hepatocyte growth factor on the transforming growth factor-beta signaling pathway

[26]. Paradoxically, galectin-7 may also induce the expression of genes known to promote cancer progression, including matrix metalloproteinase-9 (MMP-9) [27, 28]. In this case, galectin-7 expression could be induced by nuclear factor-kappa B, a transcription factor and a positive regulator of MMP-9 known to be expressed in highly aggressive tumor cells [18]. This study provides in vitro evidence suggesting not a promoting effect of galectin-7 on the chemosensitivity but a potential of galectin-7 on decreasing cell proliferation/viability, which may be an interesting topic for future studies on OSCC therapy. We also investigated the role of galectin-7 using antisense galectin-7 oligonucleotides, however, the results showed no effects of galectin-7 knockdown on cell viability. A plausible reason for this is that strongly overexpressed galectin-7 affected cell viability, whereas physiologically expressed galectin-7 did not. Therefore, the knockdown of physiologically expressed galectin-7 did not elicit a noticeable effect. Moreover, because the function of galectin-7 in the nucleus remains unclear, further studies are needed to clarify this issue.

This study suggests that low galectin-7 protein expression translates into low cumulative survival rate in patients with OSCC via tumor resistance to preoperative chemotherapy and/or radiotherapy. These data are not consistent with the findings of Saussez et al. [29], who reported that galectin-7 protein expression increases during tumor progression in hypopharyngeal and laryngeal SCC. However, this research team also reported that the percentage of cells immunopositive for galectin-7 decreased significantly with the loss of histological differentiation in hypopharyngeal SCC [30]. Furthermore, tumor progression was associated with a translocation of galectin-7 from the nucleus to the cytoplasm [29]. These data suggest that the sequestration of galectin-7 into the nucleus would prevent this protein from interfering with tumor progression or regression, leading to treatment resistance. Accordingly, a formula combining the expression level and nucleic/cytoplasmic expression ratio of galectin-7 would constitute a rational predictor of chemotherapy and/or radiotherapy resistance in patient with advanced OSCC.

Our findings suggest that the specificity of the prediction of chemotherapy and/or radiotherapy resistance using G7PS was 39.5%; therefore, there could be many false-positive results. However, one case with a response evaluation of PR who was predicted as resistant (G7PS = −0.25) died of uncontrolled neck node metastases despite surgery followed by additional radiotherapy. Therefore, patients with resistance prediction using G7PS (<0) should be considered for other treatments or drugs that were not used in this study (e.g., docetaxel or a molecular target drug). Moreover, a synergistic effect of galectin-7 and S100-A9 on cervical squamous carcinoma patients was recently reported [31]. We also identified S100-A9 as one of other potential predictive markers; therefore, identification of other useful combination markers that were not analyzed in this study may be important.

In conclusion, we identified galectin-7 as a predictor of tumor resistance and developed a predictive formula for patient survival. Accordingly, measurement of galectin-7 protein expression in fresh tissue biopsy samples at the time of diagnosis can provide invaluable information for the design of customized preoperative treatment regimens with advanced OSCC. Future challenges include the identification of other useful combination markers that were not analyzed in this study in order to improve diagnostic accuracy.

Conflict of Interest

None declared.

References

1. Warnakulasuriya, S. 2009. Global epidemiology of oral and oropharyngeal cancer. Oral Oncol. 45:309–316.
2. Kugimoto, T., K. Morita, and K. Omura. 2012. Development of oral cancer screening test by detection of squamous cell carcinoma among exfoliated oral mucosal cells. Oral Oncol. 48:794–798.
3. Carvalho, A. L., I. N. Nishimoto, J. A. Califano, and L. P. Kowalski. 2005. Trends in incidence and prognosis for head and neck cancer in the United States: a site-specific analysis of the SEER database. Int. J. Cancer 114:806–816.
4. Posner, M. R., D. M. Hershock, C. R. Blajman, E. Mickiewicz, E. Winquist, V. Gorbounova, et al. 2007. Cisplatin and fluorouracil alone or with docetaxel in head and neck cancer. N. Engl. J. Med. 357:1705–1715.
5. Vermorken, J. B., E. Remenar, C. van Herpen, T. Gorlia, R. Mesia, M. Degardin, et al. 2007. Cisplatin, fluorouracil, and docetaxel in unresectable head and neck cancer. N. Engl. J. Med. 357:1695–1704.
6. Hitt, R., A. López-Pousa, J. Martínez-Trufero, V. Escrig, J. Carles, A. Rizo, et al. 2005. Phase III study comparing cisplatin plus fluorouracil to paclitaxel, cisplatin, and fluorouracil induction chemotherapy followed by chemoradiotherapy in locally advanced head and neck cancer. J. Clin. Oncol. 23:8636–8645.
7. Yamaguchi, U., R. Nakayama, K. Honda, H. Ichikawa, T. Hasegawa, M. Shitashige, et al. 2008. Distinct gene expression-defined classes of gastrointestinal stromal tumor. J. Clin. Oncol. 26:4100–4108.
8. Negishi, A., M. Masuda, M. Ono, K. Honda, M. Shitashige, R. Satow, et al. 2009. Quantitative proteomics using formalin-fixed paraffin-embedded tissues of oral squamous cell carcinoma. Cancer Sci. 100:1605–1611.

9. Fuwa, N., T. Kodaira, K. Furutani, H. Tachibana, and T. Nakamura. 2008. A new method of selective intra-arterial infusion therapy via the superficial temporal artery for head and neck cancer. Oral Surg. Oral Med. Oral Pathol. Oral Radiol. Endod. 105:783–789.
10. Ono, M., M. Shitashige, K. Honda, T. Isobe, H. Kuwabara, H. Matsuzuki, et al. 2006. Label-free quantitative proteomics using large peptide data sets generated by nanoflow liquid chromatography and mass spectrometry. Mol. Cell. Proteomics 5:1338–1347.
11. Ono, M., M. Kamita, Y. Murakoshi, J. Matsubara, K. Honda, B. Miho, et al. 2012. Biomarker discovery of pancreatic and gastrointestinal cancer by 2DICAL: 2-dimensional image-converted analysis of liquid chromatography and mass spectrometry. Int. J. Proteomics 2012:897412.
12. Matsubara, J., M. Ono, A. Negishi, H. Ueno, T. Okusaka, J. Furuse, et al. 2009. Identification of a predictive biomarker for hematologic toxicities of gemcitabine. J. Clin. Oncol. 27:2261–2268.
13. Matsubara, J., M. Ono, K. Honda, A. Negishi, H. Ueno, T. Okusaka, et al. 2010. Survival prediction for pancreatic cancer patients receiving gemcitabine treatment. Mol. Cell. Proteomics 9:695–704.
14. Matsubara, J., K. Honda, M. Ono, S. Sekine, Y. Tanaka, M. Kobayashi, et al. 2011. Identification of adipophilin as a potential plasma biomarker for colorectal cancer using label-free quantitative mass spectrometry and protein microarray. Cancer Epidemiol. Biomarkers Prev. 20:2195–2203.
15. Matsubara, J., K. Honda, M. Ono, Y. Tanaka, M. Kobayashi, G. Jung, et al. 2011. Reduced plasma level of CXC chemokine ligand 7 in patients with pancreatic cancer. Cancer Epidemiol. Biomarkers Prev. 20:160–171.
16. Murakoshi, Y., K. Honda, S. Sasazuki, M. Ono, A. Negishi, J. Matsubara, et al. 2011. Plasma biomarker discovery and validation for colorectal cancer by quantitative shotgun mass spectrometry and protein microarray. Cancer Sci. 102:630–638.
17. Ono, M., J. Matsubara, K. Honda, T. Sakuma, T. Hashiguchi, H. Nose, et al. 2009. Prolyl 4-hydroxylation of alpha-fibrinogen: a novel protein modification revealed by plasma proteomics. J. Biol. Chem. 284:29041–29049.
18. St-Pierre, Y., C. G. Campion, andA. A. Grosset. 2012. A distinctive role for galectin-7 in cancer? Front. Biosci. 17:438–450.
19. Ito, K., K. Stannard, E. Gabutero, A. M. Clark, S. Y. Neo, S. Onturk, et al. 2012. Galectin-1 as a potent target for cancer therapy: role in the tumor microenvironment. Cancer Metastasis Rev. 31:763–778.
20. Radosavljevic, G., V. Volarevic, I. Jovanovic, M. Milovanovic, N. Pejnovic, N. Arsenijevic, et al. 2012. The roles of galectin-3 in autoimmunity and tumor progression. Immunol. Res. 52:100–110.
21. Zhu, X., M. Ding, M. L. Yu, M. X. Feng, L. J. Tan, and F. K. Zhao. 2010. Identification of galectin-7 as a potential biomarker for esophageal squamous cell carcinoma by proteomic analysis. BMC Cancer 10:290.
22. Demers, M., K. Biron-Pain, J. Hébert, A. Lamarre, T. Magnaldo, and Y. St-Pierre. 2007. Galectin-7 in lymphoma: elevated expression in human lymphoid malignancies and decreased lymphoma dissemination by antisense strategies in experimental model. Cancer Res. 67:2824–2829.
23. Demers, M., A. A. Rose, A. A. Grosset, K. Biron-Pain, L. Gaboury, P. M. Siegel, et al. 2010. Overexpression of galectin-7, a myoepithelial cell marker, enhances spontaneous metastasis of breast cancer cells. Am. J. Pathol. 176:3023–3031.
24. Critchley-Thorne, R. J., N. Yan, S. Nacu, J. Weber, S. P. Holmes, and P. P. Lee. 2007. Down-regulation of the interferon signaling pathway in T lymphocytes from patients with metastatic melanoma. PLoS Med. 4: e176.
25. Ueda, S., I. Kuwabara, and F. T. Liu. 2004. Suppression of tumor growth by galectin-7 gene transfer. Cancer Res. 64:5672–5676.
26. Inagaki, Y., K. Higashi, M. Kushida, Y. Y. Hong, S. Nakao, R. Higashiyama, et al. 2008. Hepatocyte growth factor suppresses profibrogenic signal transduction via nuclear export of Smad3 with galectin-7. Gastroenterology 134:1180–1190.
27. Park, J. E., W. Y. Chang, and M. Cho. 2009. Induction of matrix metalloproteinase-9 by galectin-7 through p38 MAPK signaling in HeLa human cervical epithelial adenocarcinoma cells. Oncol. Rep. 22: 1373–1379.
28. Saussez, S., S. Cludts, A. Capouillez, G. Mortuaire, K. Smetana, H. Kaltner, et al. 2009. Identification of matrix metalloproteinase-9 as an independent prognostic marker in laryngeal and hypopharyngeal cancer with opposite correlations to adhesion/growth-regulatory galectins-1 and -7. Int. J. Oncol. 34:433–439.
29. Saussez, S., C. Decaestecker, F. Lorfevre, D. Chevalier, G. Mortuaire, H. Kaltner, et al. 2008. Increased expression and altered intracellular distribution of adhesion/growth-regulatory lectins galectins-1 and -7 during tumour progression in hypopharyngeal and laryngeal squamous cell carcinomas. Histopathology 52:483–493.
30. Saussez, S., D. R. Cucu, C. Decaestecker, D. Chevalier, H. Kaltner, S. André, et al. 2006. Galectin 7 (p53-induced gene 1): a new prognostic predictor of recurrence and survival in stage IV hypopharyngeal cancer. Ann. Surg. Oncol. 13:999–1009.
31. Zhu, H., T. C. Wu, W. Q. Chen, L. J. Zhou, Y. Wu, L. Zeng, et al. 2013. Roles of galectin-7 and S100A9 in cervical squamous carcinoma: clinicopathological and in vitro evidence. Int. J. Cancer 132:1051–1059.

Supporting Information

Additional Supporting Information may be found in the online version of this article:

Figure S1. Infection efficiency and intracellular distribution of Ad-FLAG-GAL7. HSC3 cells were plated onto cell culture slide, infected with Ad-FLAG-GAL7, and cultured overnight with or without 1 μg/mL doxycycline. After a brief wash in PBS, the cells were fixed in 4% paraformaldehyde in PBS for 20 min at RT. After several washes in PBS, the cells were permeabilized and blocked in PBS containing 0.1% Triton X-102 and 3% bovine serum albumin (BSA) for 30 min. They were then incubated with a rabbit monoclonal anti-galectin-7 antibody (EPR4287; 1:200; LifeSpan Biosciences, Inc.) in PBS for 1 h at RT, followed by three washes with PBS. Samples were incubated for 45 min with a goat anti-rabbit IgG-TR antibody (sc-2780; 1:100; Santa Cruz Biotechnology, Inc., CA), washed three times with PBS, and the slides were mounted in 90% glycerol. Samples were then analyzed and fluorescence images were recorded using a Zeiss Axiovert 135 Fluorescence Microscope (Carl Zeiss, Oberkochen, Germany). (A) 100× magnification, bar: 100 μm. Infection efficiency was approximately 80% in HSC3 cells at MOI 50. (B) 400× magnification, bar: 20 μm. Intracellular distribution of Ad-FLAG-GAL7 is similar to IHC staining pattern of galectin-7.

Figure S2. In vitro cell viability in galectin-7 knockdown HSC2 cells. Galectin-7 (sc-44534-V) shRNA lentiviral particles and scramble control shRNA lentiviral particles-A (sc-108080) were purchased from Santa Cruz Biotechnology. Lentiviral transduction was performed in HSC2 cells. Pools of stable transductants were generated via selection with puromycin (10 μg/mL) by the manufacturer's protocol. HSC2 cells stably transduced with galectin-7-shRNA (AS) or scramble control shRNA (Cont.) were cultured in a growing medium for 60 h. (A) In vitro cell viability was determined with WST assays. No effects of galectin-7 knockdown on cell viability were observed. (B) The lysate was analyzed by Western blot analysis. Beta-actin was used as a loading control.

Clinical Translational Research

Oncology

Oncology 2014;86:94–103
DOI: 10.1159/000357408

Received: August 27, 2013
Accepted: November 8, 2013
Published online: January 18, 2014

MicroRNA Expression and Functional Profiles of Osteosarcoma

Eisuke Kobayashi[a, b] Reiko Satow[a] Masaya Ono[a] Mari Masuda[a]
Kazufumi Honda[a] Tomohiro Sakuma[c] Akira Kawai[d] Hideo Morioka[b]
Yoshiaki Toyama[b] Tesshi Yamada[a]

[a]Division of Chemotherapy and Clinical Research, National Cancer Center Research Institute, [b]Department of Orthopedic Surgery, Keio University, [c]BioBusiness Group, Mitsui Knowledge Industry and [d]Musculoskeletal Oncology Division, National Cancer Center Hospital, Tokyo, Japan

Key Words
MicroRNA · Osteosarcoma · Microarray · Proteomics

Abstract
Objective: Osteosarcoma (OS) is the most frequent primary malignant bone tumor in children and young adults. Although the introduction of combined neoadjuvant chemotherapy has significantly prolonged survival, the outcome for OS patients showing a poor response to chemotherapy is still unfavorable. In order to develop new therapeutic approaches, elucidation of the entire molecular pathway regulating OS cell proliferation would be desirable. ***Methods:*** MicroRNA (miRNA) are highly conserved noncoding RNA that play important roles in the development and progression of various other cancers. Using miRNA microarrays capable of detecting a known number of 933 miRNA, 108 miRNA were found to be commonly expressed in 24 samples of OS tissue and subjected to a cell proliferation assay. ***Results:*** We found that inhibition of 5 let-7 family miRNA (hsa-let-7a, b, f, g and i) significantly suppressed the proliferation of OS cells. Using a quantitative shotgun proteomics approach, we also found that the let-7 family miRNA regulated the expression of vimentin and serpin H1 proteins. ***Conclusions:*** Our present results indicate the involvement of let-7 family miRNA in regulation of the cell proliferation as well as epithelial-mesenchymal transition of OS. Thus, let-7 family miRNA may potentially provide novel targets for the development of therapeutic strategies against OS.

Introduction

Osteosarcoma (OS), although rare, is the most frequently occurring primary malignant bone tumor, affecting mainly the metaphysis of long bones in children and adolescents. Although the introduction of combination chemotherapy over the last 3 decades has greatly improved the 5-year survival rate of OS patients [1, 2], a significant proportion of them respond poorly to chemotherapy and have a high risk of local relapse or distant metastasis even after intensive chemotherapy and curative resection of the primary site [2]. Moreover, conven-

KARGER

E-Mail karger@karger.com
www.karger.com/ocl

0030–2414/14/0862–0094$39.50/0

Tesshi Yamada
Division of Chemotherapy and Clinical Research
National Cancer Centre Research Institute
5-1-1 Tsukiji, Chuo-ku, Tokyo 104-0045 (Japan)
E-Mail tyamada@ncc.go.jp

tional cytotoxic chemotherapeutic agents often cause nonspecific adverse events [3, 4]. To improve the outcome for OS patients, it is necessary to develop new therapeutics that target the molecular pathway regulating the proliferation of OS cells.

MicroRNA (miRNA) are small, noncoding RNA 21–25 nucleotides in length involved in various critical biological processes including development, differentiation, apoptosis and proliferation [5–7]. miRNA manipulate the function of genes through mRNA degradation and/or suppression of protein translation by binding to the 3′-untranslational region of RNA transcripts [6]. It is predicted that as many as 1,000 miRNA exist in the human genome [8], and thousands of human protein-encoding genes are collectively regulated by miRNA [9, 10]. Thus, the biological properties of miRNA may facilitate potential access to several human cancers, including rare sarcomas. In fact, it has been reported that miRNA play important roles as either tumor suppressor genes or oncogenes in several human cancers [7, 11].

To our knowledge, however, little is known about the expression and function of miRNA in OS [12–15]. Here we report, for the first time, the comprehensive profiling of miRNA expression in clinical OS samples. We also performed systemic functional screening to identify miRNA that are essential for the proliferation of OS cells, and found that inhibition of let-7 family miRNA exerted a significant suppressive effect on OS cell proliferation. In other malignancies, let-7 family miRNA have generally been considered to act as tumor suppressors. Therefore, let-7 family miRNA may provide potential targets for the development of novel therapeutic strategies against OS.

Table 1. Clinicopathological characteristics of 24 OS patients

	Number of patients	%
All	24	100
Gender		
Male	14	58.3
Female	10	41.7
Age		
<10 years	4	16.7
10–19 years	13	54.2
20–29 years	4	16.7
>30 years	3	12.5
Location		
Lower extremity	20	83.3
Upper extremity	2	8.3
Axial	2	8.3
Histological subtype		
Osteoblastic	19	79.2
Chondroblastic	2	8.3
Fibroblastic	2	8.3
Telangiectatic	1	4.2
Metastasis at diagnosis		
Absent	4	16.7
Present	20	83.3
Response to neoadjuvant chemotherapy		
Good	8	33.3
Poor	15	62.5
Not done	1	4.2
Local recurrence or distal metastasis		
Yes	9	37.5
No	15	62.5
Disease status		
CDF	12	50.0
NED	4	16.7
DOD	8	33.3

CDF = Chronic disease free; NED = no evidence of disease; DOD = dead of disease.

Patients and Methods

Patients and Tumor Samples

A total of 24 fresh frozen tissue samples from patients with OS were used in this study (table 1). All the tumor samples were obtained by diagnostic incisional biopsy from their primary sites prior to preoperative chemotherapy at the National Cancer Center Hospital (Tokyo, Japan) between 1996 and 2007, as described previously [16]. All of the patients concerned provided their written informed consent, authorizing the collection and use of their samples for research purposes. The study protocol for collection of samples was approved by the institutional review board of the National Cancer Center (Tokyo, Japan).

Cell Lines

U-2 OS, Saos-2, MNNG/HOS and MG-63 cell lines were purchased from the American Tissue Culture Collection (Manassas, Va., USA). HsOS-1, NOS-1, HuO-3N1, and HuO-9N2 cell lines were purchased from the Riken Bioresource Center Cell Bank (Tsukuba, Japan). All of the OS cell lines were cultured as recommended by the suppliers.

miRNA Microarray Analysis

Total RNA was isolated using ISOGEN (Nippon Gene, Tokyo, Japan) in accordance with the manufacturer's protocol. The quality of total RNA was assessed using an Agilent 2100 Bioanalyzer (Agilent Technologies, Palo Alto, Calif., USA). miRNA expression was profiled using 3D-Gene™ Human microRNA Oligo chips (Toray, Tokyo, Japan), onto which 939 probes and 3 negative controls were spotted in duplicate. The 939 probes represented 866 known human miRNA and 73 virus-originating miRNA (39 miRNA from Epstein-Barr virus, 17 miRNA from human cytomegalovirus and 17 miRNA from Kaposi's sarcoma-associated herpesvirus).

Real-Time RT-PCR

The relative expression level of selected miRNA was quantified by real-time RT-PCR. cDNA was obtained from 2 ng of total RNA using a TaqMan MicroRNA Reverse Transcription kit (Applied Biosystems, Foster City, Calif., USA). The TaqMan primer and probe set specific to each miRNA were designed by Applied Biosystems. Amplification data measured in triplicate as an increase in reporter fluorescence were collected using the ABI PRISM 7000 Sequence Detection System (Applied Biosystems). The values from the triplicate reactions were averaged and normalized to the level of RNU6B [17]. The relative expression levels of miRNA were calculated by the comparative threshold cycle method [18].

Anti-miR miRNA Inhibitor Screening

We designed and synthesized a library of anti-miR inhibitors for 108 miRNA commonly expressed in the 24 OS samples. Each cell line was seeded at 6,000 cells per well into opaque-walled 96-well plates in triplicate on the day before transfection to obtain 70% confluency. The cells were transfected with 9 pmol of anti-miR miRNA inhibitor per well using Lipofectamine 2000 (Invitrogen, Carlsbad, Calif., USA). Anti-miR Negative Control No. 1 (Applied Biosystems) was included in each assay plate to serve as a baseline. At 72 h after transfection, cell viability was measured using the CellTiter-Glo Luminescent Cell Viability Assay (Promega, Madison, Wisc., USA), and luminescence activity was measured with a GloMax 96 Microplate Luminometer (Promega), as described previously [19]. A 10-fold serial dilution of standard adenosine triphosphate (ATP) was included in each assay plate to calculate a standard curve. The mean ATP levels in triplicate wells were normalized to those of serially diluted standard ATP and nontargeting miRNA inhibitor (negative control) included in the same 96-well assay plates.

miRNA Transfection and Protein Extraction

U-2 OS cells were transfected with the let-7 family (7a, f, g or i) or Negative Control (No. 1 or 2) Pre-miR™ miRNA Precursor Molecule (Applied Biosystems) using Lipofectamine 2000 (Invitrogen). At 72 h after transfection, cell viability was quantified by the CellTiter-Glo Luminescent Cell Viability Assay, as described above. The attached cells were scraped out in ice-cold PBS, and centrifuged at 15,000 rpm for 10 min at 4°C to remove the supernatant. The resulting cell pellets were supplemented with 100 µl of 2% sodium deoxycholate (Wako Pure Chemical, Osaka, Japan) and vortexed [20, 21]. To 200 µl of the dissolved sample, 40 µl of 5 M urea, 10 µl of 1 M NH_4CO_3 and 1 µg of Sequencing Grade Modified Trypsin (Promega) were added. After incubation at 37°C for 20 h, this mixture was supplemented with 5% formic acid, vortexed and centrifuged at 15,000 rpm for 5 min at room temperature. The collected supernatant was treated with 240 µl of ethyl acetate, vortexed and centrifuged at 15,000 rpm for 5 min at room temperature again. After collecting 200 µl of the lower layer, the peptides it contained were dried with a SpeedVac Concentrator (Thermo Electron, Holbrook, N.Y., USA) and then dissolved in 40 µl of 0.1% formic acid. The protein concentrations of all protein samples were determined by Quant-iT™ Assay (Invitrogen).

Liquid Chromatography and Mass Spectrometry

Samples were randomized and measured in duplicate with a linear gradient of 0–80% acetonitrile in 0.1% formic acid at a speed 200 nl/min for 60 min using a nanoflow high-performance liquid chromatography system (NanoFrontier nLC; Hitachi High Technologies, Tokyo, Japan) connected to an electrospray ionization quadrupole time-of-flight mass spectrometer (Q-Tof Ultima; Waters, Milford, Mass., USA). Mass spectrometry (MS) peaks were detected, normalized and quantified, using the in-house 2-dimensional image-converted analysis of liquid chromatography and MS (2DICAL) software package, as described previously [22]. A serial identification (ID) number was applied to each MS peak detected (ID1–ID47,203).

Protein Identification by Tandem MS (MS/MS)

Peak lists were generated by the Mass Navigator software package version 1.2 (Mitsui Knowledge Industry, Tokyo, Japan) and searched against the Swiss-Prot database, release 57.5, using the Mascot software package version 2.2.1 (Matrix Science, London, UK). Trypsin was designated as the enzyme, and up to 1 missed cleavage was allowed. Initial peptide tolerances for precursor and fragment ions were ±0.8 and ±1.2 Da, respectively. To achieve $p < 0.05$, the score threshold was set by the Mascot algorithm, based on the size of the database used in this search. If a peptide was matched to multiple proteins, the protein name with the highest Mascot score was chosen.

Immunoblot Analysis

Anti-β-actin mouse monoclonal antibody (AC-74) was purchased from Sigma-Aldrich. Anti-vimentin (9E7E7) and serpin H1 (E1) mouse monoclonal antibodies were purchased from Santa Cruz Biotechnology (Santa Cruz, Calif., USA). The protein samples were subjected to SDS-PAGE and transferred to Immobilon-P membranes (Millipore, Billerica, Mass., USA). After 2 h of incubation with primary antibodies at room temperature and with the relevant secondary antibodies at room temperature for 1 h, blots were detected using enhanced chemiluminescence Western blotting detection reagents (GE Healthcare, Buckinghamshire, UK) [23].

Statistical Analysis

Statistical significance between subgroups was assessed using Welch's t test and the paired t test.

Results

miRNA Expression Profiles of OS

Global miRNA expression profiles were obtained from 24 OS samples and 8 OS cell lines. The clinicopathological features of the patients with OS are summarized in table 1. We found that 108 human-originated (online suppl. table S1; for all online suppl. material, see www.karger.com/doi/10.1159/000357408) and 2 virus-originated (hcmv-miR-UL70-3p and kshv-miR-K12-10a) miRNA were commonly expressed (>20 microarray-based arbitrary units) in all of the 24 OS samples examined, whereas 515 miRNA were not expressed (<20 units) in any of the OS samples (fig. 1a). miR-1826, miR-923, miR-1308, miR-451, miR-23a, let-7a, miR-23b, let-7c,

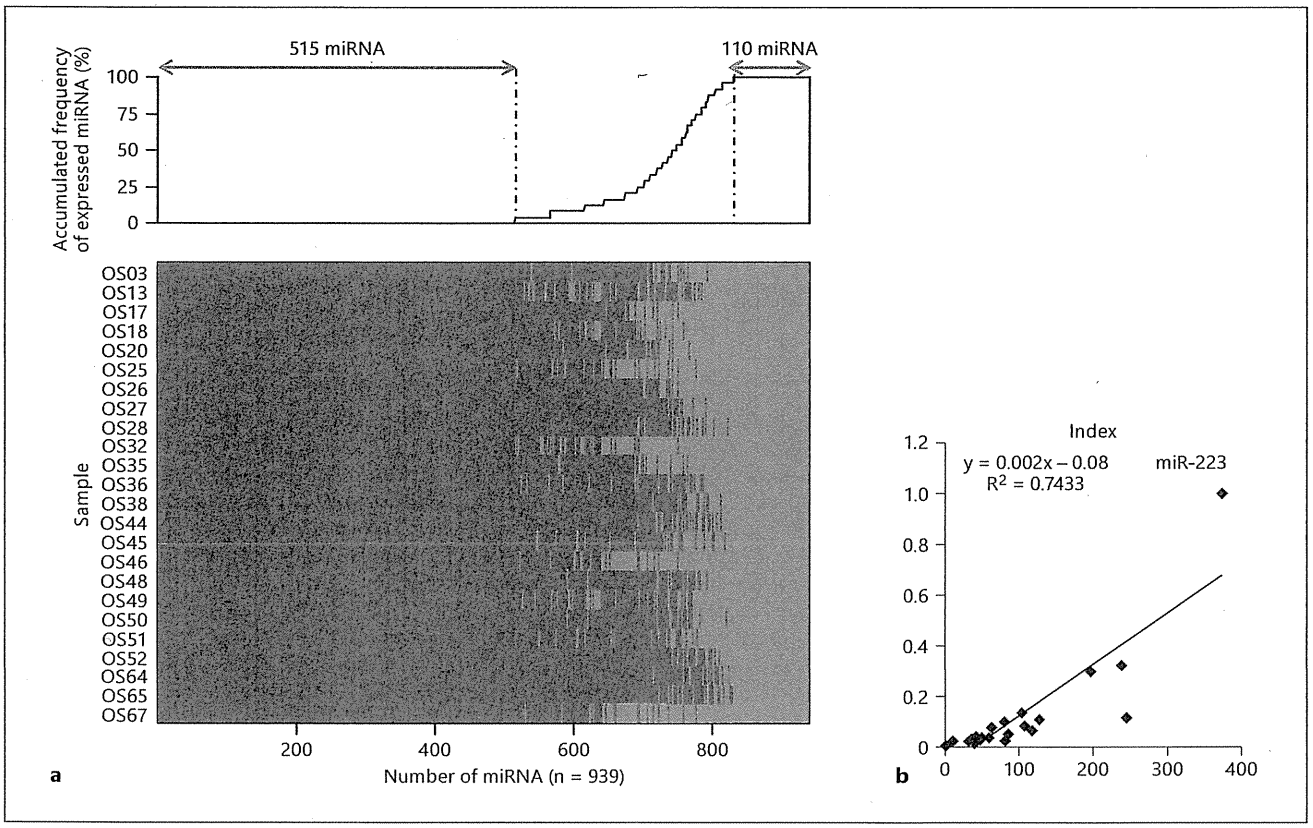

Fig. 1. Global expression of miRNA in OS. **a** The expression of 939 miRNA was examined in 24 clinical samples (range: OS03–67) using 3D-Gene miRNA microarrays. The 110 miRNA indicated by a red arrow were expressed in all the OS samples examined (>20 microarray-based arbitrary units, indicated in red columns), whereas the 515 miRNA indicated by a blue arrow were not expressed in any of them (<20 units, indicated in blue columns). **b** Correlation of miR-223 expression levels determined by microarray (x-axis, in microarray-based arbitrary units) and by quantitative real-time RT-PCR (y-axis, in arbitrary units normalized to RNU6B) in 22 OS. R = Correlation coefficient.

let-7d and miR-26a showed the highest levels of expression. The expression data on representative miRNA were also verified by real-time RT-PCR (fig. 1b and data not shown).

It was noticed that the overall profiles of miRNA expression were largely invariable among the 24 OS samples, but highly different from those of other sarcomas reported previously (data not shown), indicating that OS has an intrinsic and characteristic miRNA profile. We compared various clinicopathological characteristics, such as metastasis and prognosis, with the miRNA expression profiles. However, no definite miRNA was found to be significantly associated with the clinical behavior of the disease (data not shown), supporting the notion that OS acquires a unique miRNA expression pattern during its development.

Screening of miRNA Essential for OS Cell Proliferation

To identify miRNA essential for OS cell proliferation, we next transfected the 8 OS cell lines with synthetic inhibitors directed against the 108 miRNA of human origin, and the relative abundance of metabolically active cells was determined 72 h after transfection. The expression of the 108 miRNA and the ATP production (in percent) of the 8 OS cells transfected with these miRNA relative to control RNA are summarized in online supplementary table S1. We found that the inhibitors of 5 let-7 family miRNA (let-7a, b, f, g and i) significantly downregulated the viability of OS cells in comparison with the negative controls (fig. 2a). Conversely, the inhibitors of miR-1274a, miR-1826, miR-296-5p and miR-342-3p increased the viability of the cells. Among the 9 miRNA, the inhibitor of miR-1274a increased the average ATP pro-

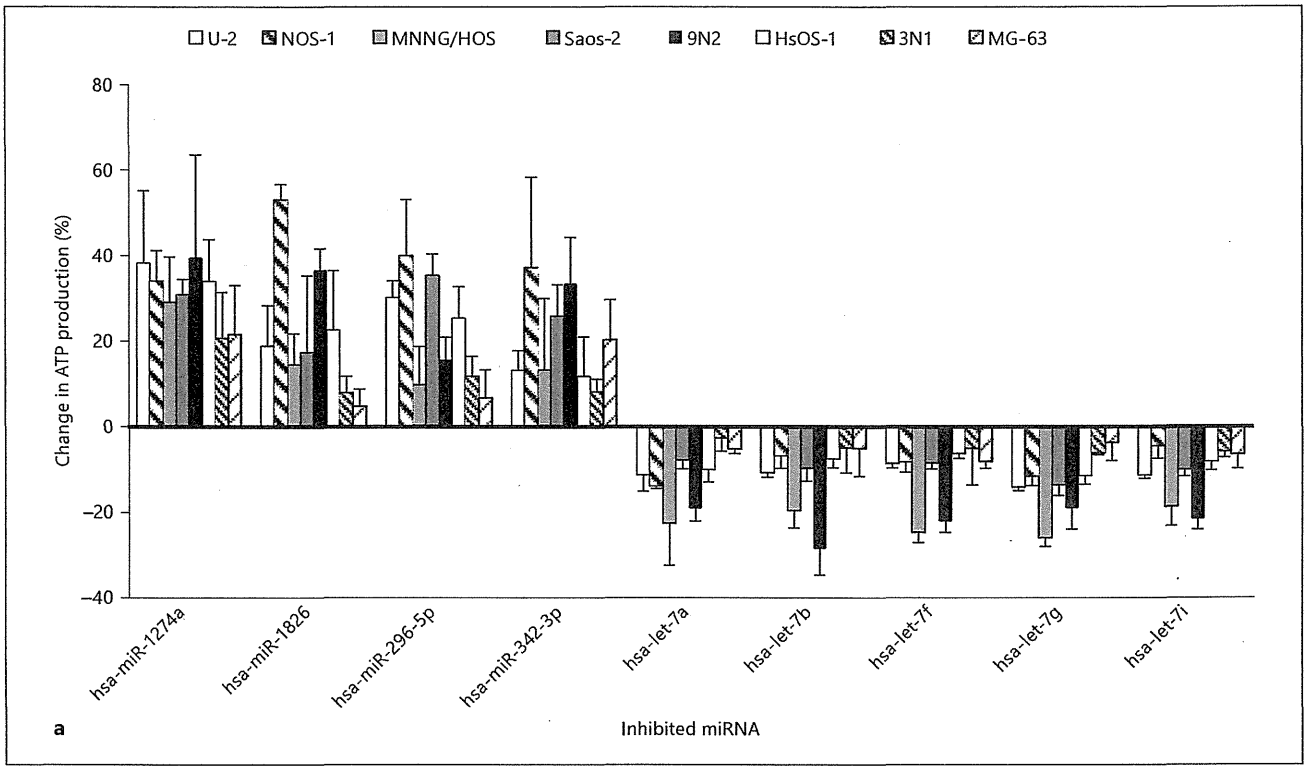

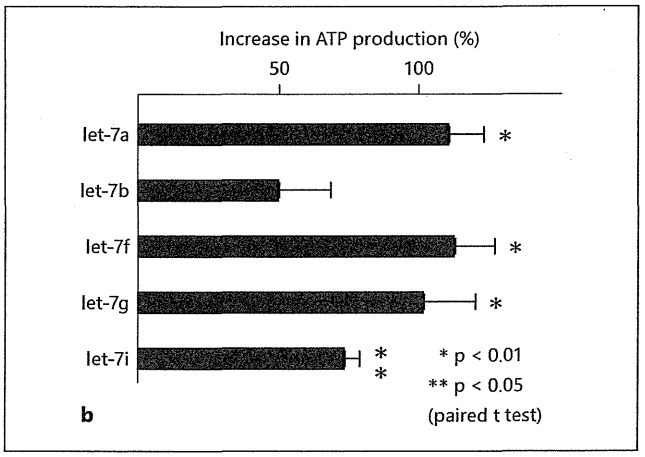

Fig. 2. Survey of miRNA regulating OS cell proliferation. **a** Percent increase (positive values) or decrease (negative values) in ATP production of 8 OS cell lines (U-2, NOS-1, MNNG/HOS, Saos-2, 9N2, HsOS-1, 3N1 and MG-63) transfected with synthetic inhibitors against miRNA. The average value of the negative control (anti-miR Negative Control No. 1) was set as 0. **b** Percent increment in ATP production in U-2 OS cells with let-7 family miRNA. The average value of the negative controls (Pre-miR miRNA Precursor Molecules, Negative Controls No. 1 and 2) was set as 0.

duction of the 8 OS cell lines (20.7–39.5% increase) and the inhibitor of let-7g reduced it (6.1–25.9% decrease; online suppl. table S1) to the maximal extent.

Transfection with let-7 Family miRNA Promotes OS Cell Proliferation

Generally, let-7 family miRNA have been considered to have tumor-suppressive functions [24]. The K-ras oncogene is one of the targets of let-7, and inhibition of let-7 increased the rate of cancer cell division, whereas overexpression of let-7 induced cell cycle arrest in the cancer cell lines [24]. However, we found that 5 of the let-7 family miRNA were commonly expressed in OS samples, and that their inhibition suppressed the viability of OS cells. To confirm these oncogenic characteristics of let-7 family miRNA in OS cells, we transfected U-2 OS cells with chemically modified, double-stranded RNA molecules designed to mimic endogenous mature miRNA of let-7a,

Table 2. Proteins regulated by let-7 family miRNA

ID	m/z	RT	Charge	Protein description	Mascot score	Peptide sequence	let-7 family	Controls	p[1]
4,893	851.0	63.7	3	serpin H1	93.14	DQAVENILVSPVVVASSLGLVSLGGK	15.24±1.96	33.31±4.41	1.71E–17
106	1,093.9	49.6	2	vimentin	73.93	EMEENFAVEAANYQDTIGR	212.34±13.97	151.14±6.40	4.30E–16
515	665.4	55.7	2	small nuclear ribonucleoprotein E	47.28	VMVQPINLIFR	86.80±5.90	62.75±2.39	3.22E–15
30,968	980.1	64.1	3	protein disulfide-isomerase	59.21	TGPAATTLPDGAAAESLVESSEVAVIGFFK	10.85±1.11	16.00±1.16	1.06E–14
324	824.4	46.6	2	heterogeneous nuclear ribonucleoprotein U	93.36	NFILDQTNVSAAAQR	114.74±9.03	75.94±8.39	3.38E–14
60	834.9	45.7	2	vimentin	54.46	ETNLDSLPLVDTHSK	267.56±19.44	195.12±7.69	3.96E–14
419	774.8	37.0	2	14-3-3 protein zeta/delta	81.66	SVTEQGAELSNEER	57.27±7.23	95.02±11.60	8.58E–14
84	867.9	44.0	2	vimentin	47.82	LQDEIQNMKEEMAR	222.70±17.28	161.62±8.15	2.53E–13
66	767.4	50.1	2	vimentin	65.19	KVESLQEEIAFLK	253.42±17.99	193.21±6.18	5.93E–13
58	794.4	39.9	2	vimentin	76.19	TNEKVELQELNDR	270.28±18.55	209.47±7.03	1.21E–12
4,771	585.9	62.9	2	vimentin	60.12	ILLAELEQLK	33.29±3.01	23.22±1.46	1.21E–12
997	759.4	55.9	3	polypyrimidine tract-binding protein 1	57.6	IAIPGLAGAGNSVLLVSNLNPER	65.10±4.57	49.00±3.38	1.57E–12
153	844.9	46.2	2	vimentin	47.24	VEVERDNLAEDIMR	171.02±14.66	124.21±5.18	2.16E–12
136	561.3	45.7	2	vimentin	52.47	EYQDLLNVK	156.93±19.07	100.58±5.15	1.20E–11
1,298	823.4	49.3	2	stress-70 protein, mitochondrial	82.19	VINEPTAAALAYGLDK	56.36±5.96	39.29±1.29	2.28E–11

Values for let-7 family and controls denote means ± SD. RT = Retention time.
[1] Welch's t test.

let-7b, let-7f, let-7g and let-7i. Again, we observed that the let-7 family miRNA significantly increased the metabolic activity of the OS cells ($p < 0.05$; fig. 2b).

Identification of Targets of let-7 Family miRNA in OS Using a Proteomics Approach

miRNA regulate the expression of target genes at the posttranscriptional level through translational inhibition as well as mRNA destabilization. One miRNA can repress the translation of hundreds of human protein-coding genes, thus exerting its distinct function. These target genes can be practically predicted, using bioinformatic approaches [10, 25, 26], but due to their relatively high rates of false positivity and negativity [6], we searched for proteins whose expression would be commonly affected by transfection with let-7 family miRNA (let-7a, let-7f, let-7g and let-7i), using an originally developed label-free quantitative MS platform: 2DICAL [22, 27].

Among a total of 47,203 independent MS peaks detected within the range of 250–1,600 m/z and within a retention time of 30–70 min, we found 253 MS peaks whose average intensity differed significantly ($p < 0.001$; Welch's t test). The intensity of 48 MS peaks was decreased in OS cells transfected with let-7 family miRNA, and that of the remaining 205 was increased. Tandem MS (MS/MS) analysis revealed that an MS peak with the highest statistical significance was derived from the *SERPINH1* (serpin H1) gene product, and the *VIM* (vimentin) gene products were detected most repeatedly (48 times) among the 253 differentially expressed MS peaks. Table 2 lists 15 MS peaks with the statistical significance of $p < 1 \times 10^{-10}$. The expression of serpin H1 was increased and that of vimentin was decreased after transfection with let-7 family miRNA. Figure 3a shows the distribution of representative serpin H1-derived and vimentin-derived MS peaks [ID 4,893 (at 851 m/z and 63.5 min) and ID 106 (at 1,094 m/z and 49.5 min), respectively] in U-2 OS cells transfected with let-7 family miRNA and controls. The differential expression and identification of serpin H1 and vimentin proteins were confirmed by immunoblotting (fig. 3b).

Discussion

Dysregulation of various miRNA has been implicated in the development and progression of human cancers. miRNA control hundreds of gene targets and play

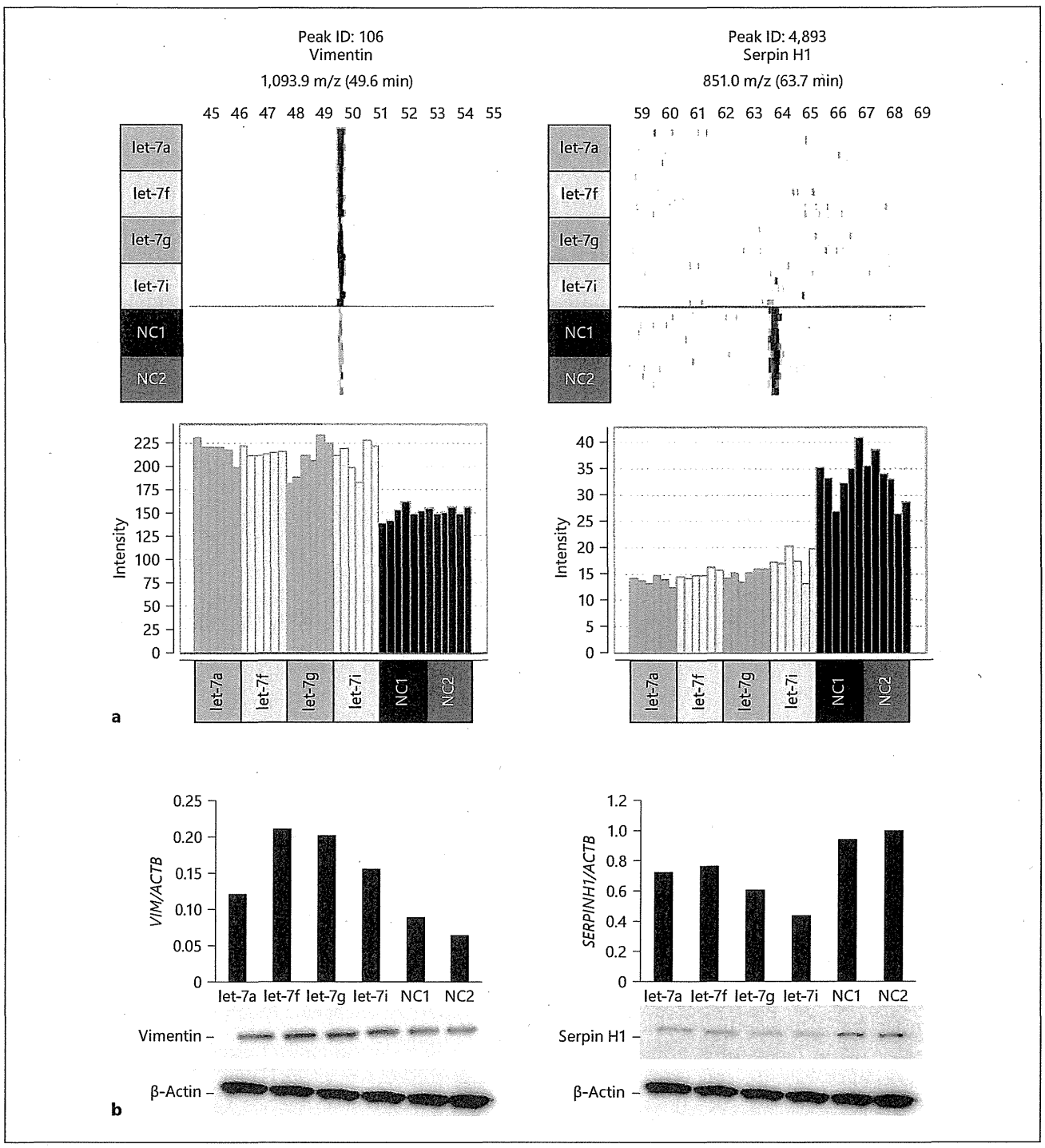

Fig. 3. Identification of proteins regulated by let-7 family miRNA. **a** Representative vimentin-derived and serpin H1-derived MS peaks detected in U-2 cells transfected with let-7 family miRNA (7a, 7f, 7g and 7i) and control RNA (NC1 and NC2). MS peaks are aligned along the retention time of liquid chromatography (in minutes). Columns: intensity (in arbitrary units) of sextuple MS peaks. **b** Detection of vimentin, serpin H1 and β-actin (loading control) in U-2 cells transfected with let-7 family miRNA (7a, 7f, 7g and 7i) and control RNA (NC1 and NC2) by immunoblotting. Columns represent the relative quantification (in arbitrary units) of vimentin *(VIM)* and serpin H1 *(SERPINH1)* normalized to β-actin *(ACTB)*.

important roles in homeostatic processes such as cell differentiation, proliferation and apoptosis [5–7]. miRNA, therefore, could be attractive candidates for the development of novel prognostic markers and/or therapeutic targets. The significance of miRNA expression has been extensively studied in various human epithelial tumors to elucidate the molecular mechanisms underlying carcinogenesis, and to identify therapeutic targets [28, 29]. However, the expression and function of miRNA in mesenchymal tumors have remained largely unknown. Subramanian et al. [30] obtained miRNA expression profiles for a series of 27 sarcomas and found distinct miRNA expression patterns for specific histopathological types, but no case of OS was included in their study. Sarver et al. [31] performed an unsupervised clustering analysis of miRNA expression in various sarcomas, including 15 cases of OS, and found that OS formed a single cluster that was distinct from other sarcomas. OS often shows a highly aggressive phenotype and lacks apparent histological differentiation, but the tissue lineage-specific regulation of miRNA expression seems to be maintained. We observed that the expression of miRNA was relatively invariable among the 24 cases of OS, regardless of their differing histological subtypes (fig. 1a). In fact we were unable to find any miRNA whose expression was significantly correlated with the clinicopathological characteristics of OS (table 1), indicating that the 108 miRNA listed in online supplementary table S1 play important roles in the development of OS.

In this study we performed an unbiased functional screening of miRNA to identify those essential for OS cell proliferation. We transfected 8 OS cell lines with miRNA inhibitors specific to the 108 miRNA commonly expressed in the 24 clinical samples, and evaluated the effects of these inhibitors on cell viability. One of the most remarkable findings was that the inhibitors of 5 let-7 family miRNA (let-7a, b, f, g and i) commonly suppressed the growth of OS cells (fig. 2a). We further confirmed these results by transfecting OS cells with let-7 family miRNA (fig. 2b). The let-7 family miRNA was originally discovered in *Caenorhabditis elegans*, and was subsequently found to be conserved in humans [32, 33]. The expression of let-7 family miRNA was reduced in various human malignancies including lung cancer, hepatocellular carcinoma, melanoma and prostate cancer [33], and the reduction in let-7 expression was associated with poor outcome in patients with lung cancer [34]. Forced expression of let-7 inhibited cell growth and downregulated multiple oncogenic proteins such as K-ras, c-Myc and HMGA2 [33, 35]. Based on these observations, let-7 family miRNA have been considered to function as tumor suppressors. However, let-7 family miRNA function differently in OS, indicating that their diverse effects are dependent on tissue lineage.

miRNA govern the expression of target proteins through mRNA degradation and suppression of protein translation [6]. Proteomics technologies have increasingly been applied for identifying the downstream targets of miRNA [36, 37]. However, the levels of alteration are often subtle and cannot be detected by conventional proteomics methods. To identify the proteins targeted by let-7 family miRNA in OS cells, we performed quantitative shotgun proteomics analysis (fig. 3a; table 2). Using the 2DICAL platform, we identified 2 let-7-responsive proteins in OS – serpin H1 and vimentin – whose expression was downregulated or upregulated, respectively, by let-7 family miRNA. In 2DICAL, whole proteins are enzymatically digested into a large array of small peptide fragments having uniform physical and chemical characteristics, and these are quantified directly by high-speed MS [22]. The 2DICAL platform is highly advantageous for clinical proteomics studies, and several cancer biomarkers have been successfully identified using this approach [27, 38, 39].

It is generally accepted that the expression of vimentin represents the mesenchymal phenotypes of various tumors, indicating that the expression of let-7 family miRNA induces OS cells to acquire mesenchymal properties, leading to an increase in tumor aggressiveness. In osteoblasts, vimentin inhibits the transactivation activity of an osteoblast-enriched transcription factor, ATF4 (activating transcription factor 4), and thus ATF4-mediated osteoblast terminal differentiation [40]. The expression of let-7 family miRNA is therefore considered to suppress the differentiation of osteoblasts and contribute to carcinogenesis. Through this osteoblast lineage-specific molecular pathway, let-7 family miRNA may exert an oncogenic function in OS cells, but not in other tumors.

Another protein that we identified as a target of let-7 family miRNA was serpin H1 (also called 'heat shock protein 47', HSP47). HSP47 is a stress-inducible collagen-binding protein that acts as a collagen-specific chaperone promoting the expression of type I collagen, which is essential for the differentiation of osteoblasts [41, 42]. Our data showed that OS cells transfected with let-7 family miRNA had reduced HSP47 expression, suggesting that this suppression of HSP47 may induce OS cells to dedifferentiate.

Conclusions

We have conducted a comprehensive functional survey of miRNA involved in the development of OS. We found that let-7 family miRNA are invariably expressed in OS and potentially contribute to OS cell proliferation and dedifferentiation. The osteoblast lineage-specific molecular pathway regulated by let-7 family miRNA could provide a novel therapeutic target for OS.

Acknowledgements

We thank Drs. Robert Nakayama and Kazutaka Kikuta (National Cancer Center Research Institute, Tokyo, Japan) for collecting samples and isolating RNA, and Ms. Sachiyo Mitani for technical assistance. E.K. is an awardee of a Research Resident Fellowship from the Foundation for Promotion of Cancer Research (Tokyo, Japan) for the Third-Term Comprehensive 10-Year Strategy for Cancer Control. Grant support was provided by the Program for Promotion of Fundamental Studies in Health Sciences conducted by the National Institute of Biomedical Innovation of Japan and the Third-Term Comprehensive Control Research for Cancer and Research on Biological Markers for New Drug Development conducted by the Ministry of Health, Labor, and Welfare of Japan.

Disclosure Statement

No potential conflicts of interest are disclosed.

References

1 Uribe-Botero G, Russell WO, Sutow WW, Martin RG: Primary osteosarcoma of bone: clinicopathologic investigation of 243 cases, with necropsy studies in 54. Am J Clin Pathol 1977;67:427–435.
2 Bielack SS, Kempf-Bielack B, Delling G, et al: Prognostic factors in high-grade osteosarcoma of the extremities or trunk: an analysis of 1,702 patients treated on neoadjuvant cooperative osteosarcoma study group protocols. J Clin Oncol 2002;20:776–790.
3 Clark JC, Dass CR, Choong PF: A review of clinical and molecular prognostic factors in osteosarcoma. J Cancer Res Clin Oncol 2008; 134:281–297.
4 Meyers PA, Schwartz CL, Krailo M, et al: Osteosarcoma: a randomized, prospective trial of the addition of ifosfamide and/or muramyl tripeptide to cisplatin, doxorubicin, and high-dose methotrexate. J Clin Oncol 2005;23: 2004–2011.
5 Ambros V: The functions of animal micro RNAs. Nature 2004;431:350–355.
6 Bartel DP: MicroRNAs: genomics, biogenesis, mechanism, and function. Cell 2004;116: 281–297.
7 Negrini M, Ferracin M, Sabbioni S, Croce CM: MicroRNAs in human cancer: from research to therapy. J Cell Sci 2007;120:1833–1840.
8 Berezikov E, Guryev V, van de Belt J, et al: Phylogenetic shadowing and computational identification of human microRNA genes. Cell 2005;120:21–24.
9 Lewis BP, Burge CB, Bartel DP: Conserved seed pairing, often flanked by adenosines, indicates that thousands of human genes are microRNA targets. Cell 2005;120:15–20.
10 Lim LP, Lau NC, Garrett-Engele P, et al: Microarray analysis shows that some micro RNAs downregulate large numbers of target mRNAs. Nature 2005;433:769–773.
11 Zhang B, Pan X, Cobb GP, Anderson TA: microRNAs as oncogenes and tumor suppressors. Dev Biol 2007;302:1–12.
12 Song B, Wang Y, Xi Y, et al: Mechanism of chemoresistance mediated by miR-140 in human osteosarcoma and colon cancer cells. Oncogene 2009;28:4065–4074.
13 Song B, Wang Y, Titmus MA, et al: Molecular mechanism of chemoresistance by miR-215 in osteosarcoma and colon cancer cells. Mol Cancer 2010;9:96.
14 Ziyan W, Shuhua Y, Xiufang W, Xiaoyun L: MicroRNA-21 is involved in osteosarcoma cell invasion and migration. Med Oncol 2011; 28:1469–1474.
15 He C, Xiong J, Xu X, et al: Functional elucidation of MiR-34 in osteosarcoma cells and primary tumor samples. Biochem Biophys Res Commun 2009;388:35–40.
16 Kobayashi E, Masuda M, Nakayama R, et al: Reduced argininosuccinate synthetase is a predictive biomarker for the development of pulmonary metastasis in patients with osteosarcoma. Mol Cancer Ther 2010;9:535–544.
17 Fukao T, Fukuda Y, Kiga K, et al: An evolutionarily conserved mechanism for microRNA-223 expression revealed by microRNA gene profiling. Cell 2007;129:617–631.
18 Huang L, Shitashige M, Satow R, et al: Functional interaction of DNA topoisomerase IIα with the β-catenin and T-cell factor-4 complex. Gastroenterology 2007;133:1569–1578.
19 Yamaguchi U, Honda K, Satow R, et al: Functional genome screen for therapeutic targets of osteosarcoma. Cancer Sci 2009;100:2268–2274.
20 Masuda T, Tomita M, Ishihama Y: Phase transfer surfactant-aided trypsin digestion for membrane proteome analysis. J Proteome Res 2008;7:731–740.
21 Ono M, Matsubara J, Honda K, et al: Prolyl 4-hydroxylation of α-fibrinogen: a novel protein modification revealed by plasma proteomics. J Biol Chem 2009;284:29041–29049.
22 Ono M, Shitashige M, Honda K, et al: Label-free quantitative proteomics using large peptide data sets generated by nanoflow liquid chromatography and mass spectrometry. Mol Cell Proteomics 2006;5:1338–1347.
23 Idogawa M, Masutani M, Shitashige M, et al: Ku70 and poly(ADP-ribose) polymerase-1 competitively regulate β-catenin and T-cell factor-4-mediated gene transactivation: possible linkage of DNA damage recognition and Wnt signaling. Cancer Res 2007;67:911–918.
24 Osada H, Takahashi T: let-7 and miR-17-92: small-sized major players in lung cancer development. Cancer Sci 2011;102:9–17.
25 Lewis BP, Shih IH, Jones-Rhoades MW, et al: Prediction of mammalian microRNA targets. Cell 2003;115:787–798.
26 Krek A, Grun D, Poy MN, et al: Combinatorial microRNA target predictions. Nat Genet 2005;37:495–500.
27 Negishi A, Ono M, Handa Y, et al: Large-scale quantitative clinical proteomics by label-free liquid chromatography and mass spectrometry. Cancer Sci 2009;100:514–519.
28 Lu J, Getz G, Miska EA, et al: MicroRNA expression profiles classify human cancers. Nature 2005;435:834–838.
29 Volinia S, Calin GA, Liu CG, et al: A micro RNA expression signature of human solid tumors defines cancer gene targets. Proc Natl Acad Sci USA 2006;103:2257–2261.
30 Subramanian S, Lui WO, Lee CH, et al: MicroRNA expression signature of human sarcomas. Oncogene 2008;27:2015–2026.
31 Sarver AL, Phalak R, Thayanithy V, Subramanian S: S-MED: sarcoma microRNA expression database. Lab Invest 2010;90:753–761.

32 Roush S, Slack FJ: The let-7 family of micro RNAs. Trends Cell Biol 2008;18:505–516.
33 Boyerinas B, Park SM, Hau A, et al: The role of let-7 in cell differentiation and cancer. Endocr Relat Cancer 2010;17:F19–F36.
34 Takamizawa J, Konishi H, Yanagisawa K, et al: Reduced expression of the let-7 micro RNAs in human lung cancers in association with shortened postoperative survival. Cancer Res 2004;64:3753–3756.
35 Lee YS, Dutta A: The tumor suppressor microRNA let-7 represses the HMGA2 oncogene. Genes Dev 2007;21:1025–1030.
36 Baek D, Villen J, Shin C, et al: The impact of microRNAs on protein output. Nature 2008; 455:64–71.
37 Selbach M, Schwanhausser B, Thierfelder N, et al: Widespread changes in protein synthesis induced by microRNAs. Nature 2008;455:58–63.
38 Matsubara J, Ono M, Negishi A, et al: Identification of a predictive biomarker for hematologic toxicities of gemcitabine. J Clin Oncol 2009;27:2261–2268.
39 Matsubara J, Ono M, Honda K, et al: Survival prediction for pancreatic cancer patients receiving gemcitabine treatment. Mol Cell Proteomics 2010;9:695–704.
40 Lian N, Wang W, Li L, et al: Vimentin inhibits ATF4-mediated osteocalcin transcription and osteoblast differentiation. J Biol Chem 2009;284:30518–30525.
41 Ragg H: The role of serpins in the surveillance of the secretory pathway. Cell Mol Life Sci 2007;64:2763–2770.
42 Nagai N, Hosokawa M, Itohara S, et al: Embryonic lethality of molecular chaperone Hsp47 knockout mice is associated with defects in collagen biosynthesis. J Cell Biol 2000; 150:1499–1506.

Alternative Mammalian Target of Rapamycin (mTOR) Signal Activation in Sorafenib-resistant Hepatocellular Carcinoma Cells Revealed by Array-based Pathway Profiling*[S]

Mari Masuda‡§, Wei-Yu Chen¶, Akihiko Miyanaga‡, Yuka Nakamura‡, Kumiko Kawasaki‖, Tomohiro Sakuma‖, Masaya Ono‡, Chi-Long Chen¶, Kazufumi Honda‡, and Tesshi Yamada‡

Sorafenib is a multi-kinase inhibitor that has been proven effective for the treatment of unresectable hepatocellular carcinoma (HCC). However, its precise mechanisms of action and resistance have not been well established. We have developed high-density fluorescence reverse-phase protein arrays and used them to determine the status of 180 phosphorylation sites of signaling molecules in the 120 pathways registered in the NCI-Nature curated database in 23 HCC cell lines. Among the 180 signaling nodes, we found that the level of ribosomal protein S6 phosphorylated at serine residue 235/236 (p-RPS6 S235/236) was most significantly correlated with the resistance of HCC cells to sorafenib. The high expression of p-RPS6 S235/236 was confirmed immunohistochemically in biopsy samples obtained from HCC patients who responded poorly to sorafenib. Sorafenib-resistant HCC cells showed constitutive activation of the mammalian target of rapamycin (mTOR) pathway, but whole-exon sequencing of kinase genes revealed no evident alteration in the pathway. p-RPS6 S235/236 is a potential biomarker that predicts unresponsiveness of HCC to sorafenib. The use of mTOR inhibitors may be considered for the treatment of such tumors. ***Molecular & Cellular Proteomics 13: 10.1074/mcp.M113.033845, 1429–1438, 2014.***

Hepatocellular carcinoma (HCC)[1] is the third most common cause of cancer-related death worldwide (1). Advanced HCC often cannot be managed with local treatments (surgical resection, ethanol injection, radiofrequency ablation, chemoembolization), but no systemic chemotherapy with conventional cytotoxic agents had been shown to be effective until a landmark phase III clinical trial (the Sorafenib HCC Assessment Randomized Protocol) revealed significant survival prolongation in patients treated with sorafenib (Nexavar; Bayer Healthcare Pharmaceuticals Inc. Berlin, Germany) (2). Furthermore, it has been reported that some patients show remarkable tumor shrinkage after short-term administration of sorafenib (3). Based on these results, sorafenib monotherapy has been employed as the current standard first-line treatment for unresectable HCC. However, not all HCC patients show the desired therapeutic benefits of sorafenib. The overall survival prolongation of unselected patients in the SHARP trial was limited to 2.8 months (2), and an objective tumor response was observed only in a small proportion of patients (0.6% to 2%) (2, 4). Given the relatively high cost and occasional severe adverse events (diarrhea, hand-foot skin reaction, hypertension, and others) (2, 4), there is an urgent need to identify a predictive biomarker that could exclude advanced HCC patients who are unlikely to benefit from sorafenib therapy.

Sorafenib is a multi-kinase inhibitor that blocks tumor cell proliferation and angiogenesis through the inhibition of c-RAF and b-RAF, as well as many receptor tyrosine kinases, including vascular endothelial growth factor receptors 2 and 3, platelet-derived growth factor receptor-α, Fms-related tyrosine kinase 3, RET, and c-KIT (5). In view of this broad inhibitory spectrum, the precise mechanisms underlying the anti-

From the ‡Division of Chemotherapy and Clinical Research, National Cancer Center Research Institute, Tokyo, 104-0045 Japan; ¶Department of Pathology, Wan Fan Hospital and Taipei Medical University, Taipei, 11031 Taiwan; ‖BioBusiness Group, Mitsui Knowledge Industry, Tokyo, 164-8555 Japan

Received August 23, 2013, and in revised form, February 2, 2014
Published, MCP Papers in Press, March 18, 2014, DOI 10.1074/mcp.M113.033845
Author contributions: M.M. and T.Y. designed research; M.M., W.C., A.M., and Y.N. performed research; M.M. and K.K. contributed new reagents or analytic tools; M.M., W.C., K.K., T.S., and C.C. analyzed data; M.M. and T.Y. wrote the paper; M.M. developed the methodology; M.O. and K.H. contributed to the conception of the study; T.Y. supervised research.

[1] The abbreviations used are: HCC, hepatocellular carcinoma; ERK, extracellular signal-regulated kinase; IC_{50}, half-maximal (50%) inhibitory concentration; p-RPS6 S235/236, ribosomal protein S6 phosphorylated at the serine 235/236 residue; MAPK, mitogen-activated protein kinase; RPPA, reverse-phase protein array; mTOR, mammalian target of rapamycin; RSK, 90-kDa ribosomal protein S6 kinase; S6K, 70-kDa ribosomal protein S6 kinase.